

BIOMECHANICAL ANALYSIS OF ENTRY, EGRESS AND LOADING OF A PASSENGER VEHICLE WITH REAR HINGED REAR DOORS

James Shippen¹

¹ Department of Industrial Design, Coventry University, Priory Street, Coventry CV1 5FB, United Kingdom

Received 28 November 2011; accepted 1 March 2012

Abstract: A biomechanical analysis was undertaken to establish the articulation of the back lumbar region and the loads in the muscles of the back during entry and egress of a passenger vehicle with both forwarded hinged and rear hinged doors. The study was then extended to consider placing an object and retrieving an object from the rear seat of passenger vehicles with either forwarded hinged or rear hinged doors. It was found that loads in the muscles of the back and articulation angles were lower for the vehicle equipped with rear hinged doors than for the same activity in the same model of vehicle with forwarded hinged doors.

Keywords: biomechanical analysis, full body model, muscle modeling, rear hinged doors, coach doors.

1. Introduction

It is widely assumed that rear-hinged doors make entering and exiting domestic passenger vehicles easier although little research has been undertaken to quantitatively verify this assumption. The new model of the Meriva from Vauxhall/General Motors launched in 2010 features a combination of conventional forwarded hinged front doors and rear hinged rear doors for access by the rear passengers. These rear doors open to an angle of 84° rather than the 68° on the conventionally hinged doors found on the previous models of this model. An electronic device prevents the rear door from unlatching the front door is latched or while the vehicle is in motion. This design is called the FlexDoor system by General Motors. The rationale for this arrangement is that a rear occupant can enter the vehicle in a natural way, walking forward toward the vehicle and turning to sit, and

then can exit by stepping forward out of the vehicle. Additionally, this configuration aids the loading and off-loading of children into the rear seats by adults in the front seats as the open front and rear doors form a secure area adjacent to the vehicle. Additionally, a handle on the B-pillar allows the occupant to lower themselves backwards into the car.

The objective of this study was to assess the lower back injury risk for users during entry, egress and placing objects on the rear seat of the Meriva with the FlexDoor system versus a conventional rear door. Large intervertebral forces and asymmetric loading in combination with lower back articulations are known contributors to spinal injury (Chow et al., 2005; Cooper and Ghassemieh, 2007). Therefore, the study measured the articulations of the lumbar region of the back and calculated the loads in the muscles surrounding the spine during these operations.

¹ Corresponding author: aa2388@coventry.ac.uk

2. Methods

A 12 camera Vicon 3-dimensional optical tracking system (Vicon Instruments, Oxford, UK) was used to measure the movement of subjects as they entered and exited from the base model Meriva, with front hinged rear doors and the new model Meriva, with rear hinged rear doors. This procedure required retro-reflective markers to be attached to the subject at pre-defined anatomical landmarks (Fig. 1). The subject and vehicle is then surrounded by a number of cameras at known locations which have a light source next to the lens and a high contrast filter embedded in the opto-electrics. This results in the camera only sensing the markers attached to the subject and not the subject themselves which reduces the complexity of the visual field. Therefore, following a calibration exercise, the 2-dimensional images returned to a central processor by each of the 12 cameras can be reconstructed into a single model of the markers in 3-dimensional space (Grimshaw et al., 1998). In this study, the location of the marker can be measured with an error of less than 1mm. If the locations of the markers are measured, the position of the subject can be inferred.

This procedure is normally used to measure the movement of subjects in a clinical environment where there is little obstruction between the subject and the cameras. This is not the case for the current study as the subject had to enter and exit the vehicle and place objects on the rear seat during which the vehicle could cause many of the markers on the subject to become unsighted by the cameras. For the 3-dimensional reconstruction of the location of a marker it is necessary for at least 2 cameras to simultaneously sight each marker. To maximise the visibility of the markers to the cameras, the 12 cameras



Fig. 1.
A Subject with Retro-Reflective Markers Attached for 3-Dimensional Optical Tracking

were positioned around and close to the vehicle with the all the doors and tailgate in the open position (Fig. 2). Numerous trials were undertaken prior to data collection to optimise the positioning of the camera and maximise the visibility of the markers.



Fig. 2.
The Test Vehicle Surrounded by 3-Dimensional Optical Tracking Cameras

To calculate the flexion/extension, lateral bending and axial rotation of the lumbar spine, co-ordinate systems were defined for the pelvis and the upper thorax using the positions of the markers attached to those respective anatomical regions. The origin of the pelvic system was defined as the midpoint between the right and left anterior, superior iliac spines. The y-axis of the pelvic co-ordinate system was defined as the line from the origin to the left anterior, superior iliac spine. The xy plane of the pelvic system was defined as the plane containing the y-axis and the midpoint between the right and left posterior, superior iliac spines. The origin of the thoracic co-ordinate system was defined as the clavicle notch on the sternum. The z-axis was defined as parallel to the line connecting the tips of the spinal process on the C7 and T10 vertebrae. The xz plane was defined as a plane containing the y-axis and the xiphoid process.

The lumbar spine articulations are then calculated as the rotation of thoracic co-ordinate system relative to the pelvic co-ordinate system as described in the Appendix 1.

It is impractical to directly measure the loads in the muscles of the back therefore a biomechanical model consisting of jointed rigid segments and force generating muscles (Fig. 3). A mechanical model of a human was constructed. The model consisted of 31 segments representing the major anatomical components (head, thorax, pelvis, upper/lower arms, hands, upper/lower legs, feet, scapulae, clavicles, seven cervical and five lumbar vertebrae). The mass distribution and inertia properties of the segments were obtained from Hatze (1980). These segments were connected with 35 joints. The joints were modelled by constraint equations which enabled movement of the unconstrained generalized co-ordinates at the joints, and

thus represent the function of the anatomical counterpart, e.g. a spherical joint for the hip joint, a hinge joint for the elbow, a two-axis cylindrical joint for the ankle, a slide joint for scapula/thorax, a roll/slide joint for the knee.

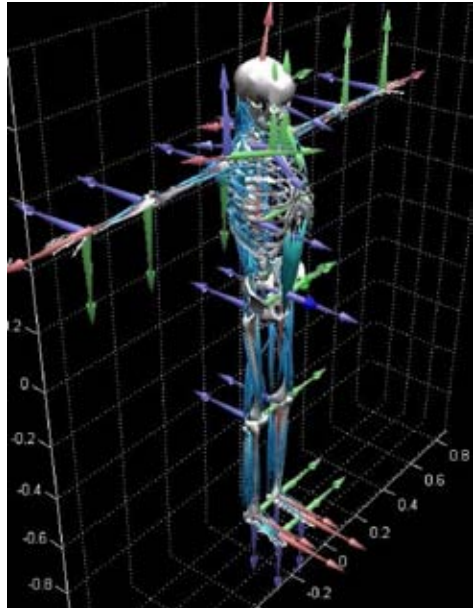


Fig. 3.
The Biomechanical Model

A muscle's force generating ability is a function of its physiological cross-sectional area (PCSA) (Brand et al., 1986) at optimal muscle length which has been defined as the muscle volume divided by the optimal fiber length, where the muscle volume was defined as muscle mass divided by its density (Breteler et al., 1999). There is a strong positive correlation between the cross-sectional area of a muscle and its maximal force output - i.e. the larger the PCSA of a muscle, the more force it can produce (Lehmkuhl et al., 1988). The maximal isometric force is assumed to be the product of the muscles' PCSA and maximal muscle stress. Von-Recklinghausen (1920) reported the stress to be 0.36N/mm^2 and

Haxton (1944) reported the absolute muscle stress to be 0.39N/mm^2 . Therefore, a maximal stress of 0.37N/mm^2 was implemented in the model.

The motion of the above system is described by Lagrange's equation (Eq. (1)):

$$Q_i = \frac{d}{dt} \left(\frac{\partial T}{\partial \dot{q}_i} \right) - \frac{\partial T}{\partial q_i} + \frac{\partial U}{\partial q_i} \quad (1)$$

where:

q_i = the i^{th} generalized co-ordinate

Q_i = the generalized force applied to the i^{th} generalized co-ordinate

T = the kinetic energy of the dancer

U = the potential energy of the dancer.

For this study, generalized co-ordinates predominantly represent the articulation of the dancers' joints, and the generalized forces are predominantly the torques produced by the muscles at the corresponding joints. Therefore, given the joint articulation histories, the external torques and a mass distribution model, the torques at the joints were being calculated.

The sum of the external forces acting on the subject was calculated by considering the acceleration of the centre of mass; this external force was applied to the biomechanical model at the points of external contact. For multiple contacts, a consideration of angular acceleration of the subject was used to calculate the force distribution amongst the contact points.

The time histories of the joint articulations were derived from marker positional data

recorded by a 12-camera Vicon MX40 three-dimensional passive optical tracking system (Vicon UK, Oxford, UK). Thirty-seven retro-reflective markers were attached to the subject at anatomical landmarks (Fig. 1), which could represent the whole body movement of the subject. The motion data were recorded at 125 frames per second. Having recorded the location of the markers attached to the subjects, the joint articulation time histories and their time derivatives were calculated and expressed as moving-axis Euler angles using a script written in the Vicon processing macro-language BodyLanguage. Cubic interpolation splines were fitted to the recorded articulation data, ensuring continuity in the angular second-order time derivative. The interpolation splines for the joint articulations were then applied to the musculoskeletal model. Lagrange's equation was then used to calculate the torques at the joints.

Each joint in the body is traversed by numerous muscles that contribute to the torques experienced at the joint. The number of muscles considered in the current study is 196, divided into 539 muscle units, contributing to 53 torques at joints throughout the body. The muscles were modelled as force generators acting between their respective origins and insertions. Muscle paths were also modelled, when appropriate, as passing over intermediate anatomical locations; for example, sartorius has its origin in the pelvis, inserts into the tibia, and passes over an intermediate point on the femur. Muscles with multiple or distributed origins and insertions were modelled as discrete muscle units. For example, biceps femoris has two origins, one on the pelvis and a second on the femur, inserts into the head of the fibula, and is split in two by the lateral collateral ligament. Hence, this muscle was represented as two

distinct muscle units. The model consisted of 539 muscle units in 196 distinct muscles. The isometric maximal force for each muscle was derived from numerous sources (Pierrynowski and Morrison, 1985; Von-Voss, 1956; Brand et al., 1982).

As the number of muscles is greatly in excess of the number of torques at the joints, there is not a unique solution for the loads in the muscles that result in the observed torque distribution. Therefore, it is necessary to select one solution from the infinite number of possible solutions that minimizes an optimization function. Numerous optimization functions have been proposed (An et al., 1984; Gracovetsky et al., 1977; Brand et al., 1982). For the current study, the sum of the square of the muscle activations is minimized, where muscle activation is defined as the muscle force divided by the muscle maximal isometric force (Zajac, 1989). This function was selected because it has the effect of reducing the maximum muscle activation, which will reduce the propensity to fatigue, and hence the function can be physiologically justified (Erdemir et al., 1989). The optimized solution must also satisfy a set of equality conditions (the torques due to external forces and segmental inertial forces must equal the torque due to the surrounding muscles at each joint) and inequality conditions (the load in each muscle must be positive, as the muscle cannot push, and the load must be less than the maximum force the muscle can generate).

The above optimization conditions are summarized as follows (Eq. (2)):

Minimize optimization function =

$$\sum_{i=1}^n \left(\frac{F_i}{F_{0i}}\right)^2 \quad (2)$$

where:

n = the number of muscles

F_i = the magnitude of the instantaneous force developed in the i^{th} muscle

F_{0i} = the maximal isometric force for the i^{th} muscle

$\frac{F_i}{F_{0i}}$ = activation of the i^{th} muscle

subject to equality constraints applied to the torques at the joints (Eq. (3)):

$$\mathbf{T}_k = \sum_{i=1}^m ((\mathbf{r}_i - \mathbf{p}_k) \times \mathbf{F}_i) \quad (3)$$

where:

\mathbf{T}_k = torque vector associated with a degree of freedom of the k^{th} joint

m = number of muscles acting across the k^{th} joint

\mathbf{r}_i = position vector of the origin of i^{th} muscle segment

\mathbf{p}_k = position vector of the k^{th} joint center

\mathbf{F}_i = force vector of the i^{th} muscle

and subject to inequality constraints:

$F_i > 0$ (i.e., the muscle cannot push)

$F_i < F_{\text{max}_i}$

where F_{max_i} = magnitude of maximum force capable of being developed by the i^{th} muscle.

The above optimization was solved for the muscle forces, F_i , in Matlab® using a least squares Levenberg-Marquardt method (Levenberg, 1944; Marquardt, 1963). For

this study it was decided to calculate the loads in the erector spinae muscles which are situated in the lumbar region of the back and the rhomboid major muscles in the thoracic region of the back.

Twelve subjects were recruited for the trials ranging in height from 1.52 m to 1.85 m, ages from 18 to 60 and both genders. The subjects were instructed to:

1. Enter the car and sit on the rear seat on the side of the vehicle closest to the point of entry.
2. Exit the car from the rear seat via the door closest to their seating place.
3. Place a bag with handles weighing 5 kg on the rear seat of the vehicle on the side of the vehicle closest to them.
4. Retrieve a bag with handles weighing 5 kg from the rear seat of the vehicle which has been placed on the side of the vehicle closest to them.

The above trials were conducted three times by all subjects with the vehicle with forward hinged rear doors and rear hinged rear doors. All data was filtered with a low pass 4th order Butterworth filter with a 20 Hz cut-off frequency.

3. Results

Examples of the motion capture and muscle modeling can be seen at:

- www.marlbroom.com/bag_in.wmv (1.3Mb);
- www.marlbroom.com/bag_out.wmv (4.5Mb);
- www.marlbroom.com/sit_in.wmv (4.8Mb);
- www.marlbroom.com/sit_out.wmv (3.8Mb).

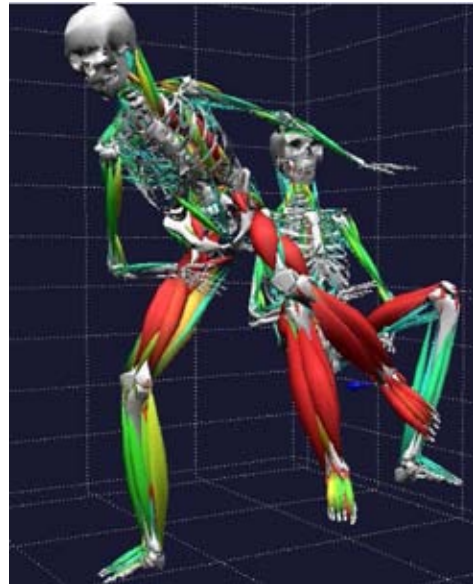


Fig. 4.
An Example of Muscle Activations During Vehicle Egress

Fig. 4 shows an example of the muscle activation distribution calculated during vehicle egress. Fig. 5 shows examples of back flexion/extension, lateral bending and axial rotation of the lumbar spinal region for one subject during the vehicle entry, egress, bag placement and bag retrieval tasks.

The peak values of the back flexion/extension, lateral bending and axial rotation of the lumbar spinal region were recorded for each subject during each trial for both vehicles. The percentage changes of these rotations between the front hinged and rear hinged vehicles was then calculated for each vehicle and the average across the sampled population is shown in Table 1. A negative value indicates that a smaller rotation was required for the task associated with the rear hinged rear doors.

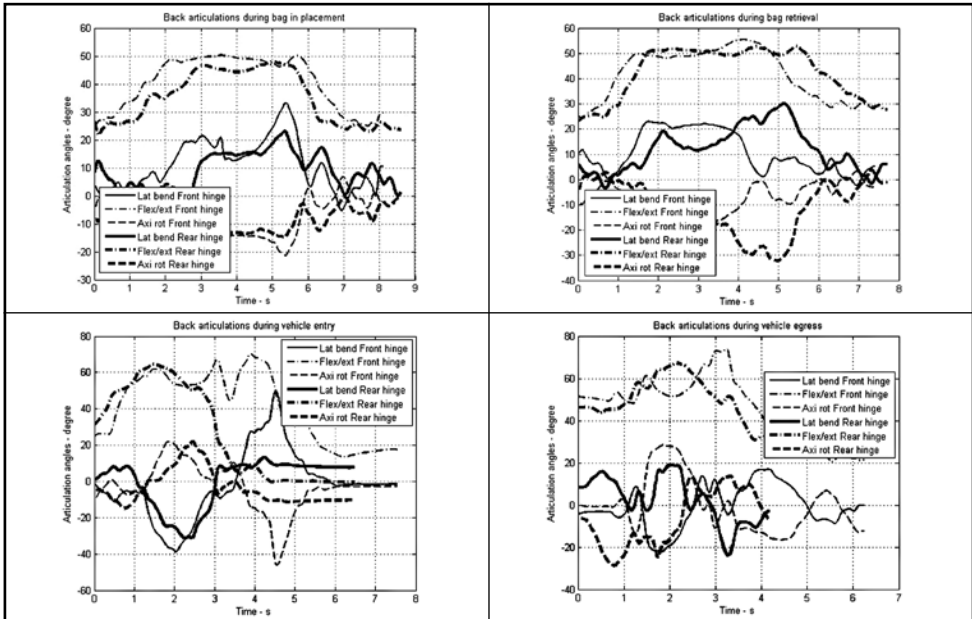


Fig. 5. Examples of Back Flexion/Extension, Lateral Bending and Axial Rotation of the Lumbar Spinal Region for One Subject During the Vehicle Entry, Egress, Bag Placement and Bag Retrieval Tasks

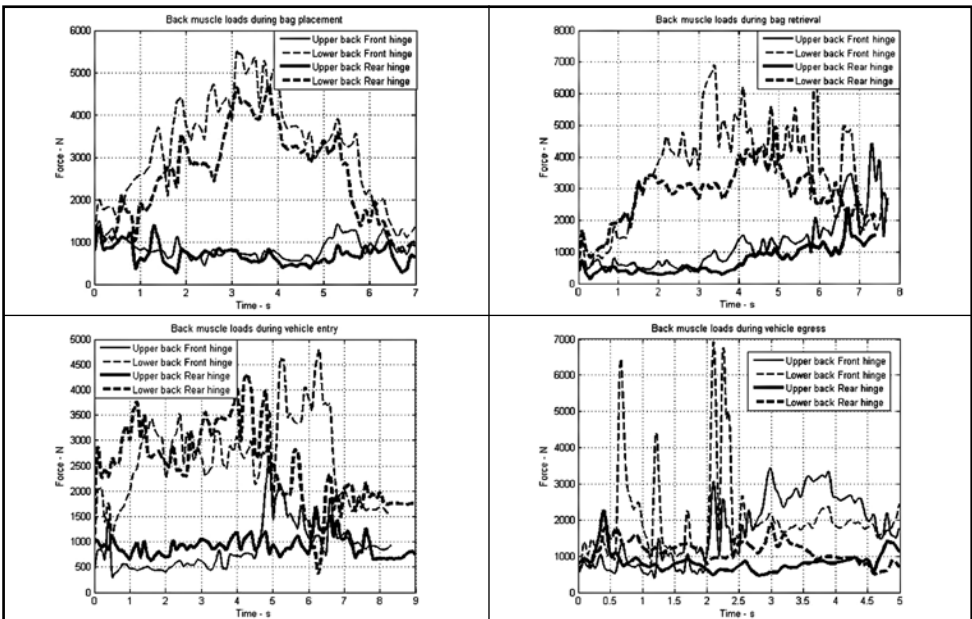


Fig. 6. Examples of Loads in the Upper and Lower Back Regions for One Subject During the Vehicle Entry, Egress, Bag Placement and Bag Retrieval Tasks

Table 1*Change in Lumbar Spine Articulation from Forward Hinged Doors to Rear Hinged Doors*

	Change in flexion/ extension	Change in lateral bending	Change in axial rotation
Bag in	-8°	6°	-6°
Bag out	-13°	4°	-13°
Vehicle entry	-31°	10°	-24°
Vehicle egress	-1°	-7°	-4°

The peak values in the erector spinae muscles and the rhomboid major muscles calculated for each subject during each trial for both vehicles and the percentage changes of these forces between the front hinged and rear hinged vehicles was then calculated for each vehicle and the average is shown in Table 2. A negative value indicates that a smaller load was occurred during the task associated with the rear hinged rear doors.

The flexion/extension and axial rotation of the lumbar region of the back decreased for all tasks for the rear hinged doors relative to the forward hinged doors of the original vehicle design. This is because the region of the body inferior to the lumbar region can be placed in a posture more aligned to the required articulation direction due to wider opening door and less intrusive positioning of the door.

Table 2*Change in Back Muscle Loading from Forward Hinged Doors to Rear Hinged Doors*

	Change in peak erector spinae force	Change in rhomboid major force
Bag in	-20%	-20%
Bag out	-18%	-54%
Vehicle entry	-30%	-6%
Vehicle egress	-15%	-21%

4. Conclusions

It has been shown that it is possible to collect 3-dimensional movement data from inside a passenger vehicle using an optical tracking system. However, the positioning of the cameras is critical to the success of the task and correct positioning is difficult to determine. If full body motion data is not required it is recommended that optical tracking only relates to the sub region of the body which is of interest as this will considerably ease the data collection task.

The loads in the thoracic and lumbar regions of the back decreased for all trials with the rear hinged doors relative to the front hinged doors. The larger reduction in load occurred in the rhomboid major muscles during the bag removal task. This was due to the large opening angle of the door enabling the subjects to adopt a posture which reduced the bending moment on the back. The reduction in the back loading during vehicle entry and egress is due to the subjects using the B-post pillar handle to provide a counter moment on the back.

The biomechanical analysis of the rear hinged rear door was undertaken at a stage in the design process after the decision to commit to this configuration had been taken. It would have been possible, and potentially preferable, to apply the technique earlier in the design process during conceptual design. This would require the construction of mock-up bucks in which participants of the trials would undertake tasks whilst being recorded in a motion laboratory.

Appendix 1

CALCULATION OF ANGLES BETWEEN CO-ORDINATE SYSTEMS ROTATED ABOUT FLOATING AXES

The rotation of a vector \mathbf{p} about the x-axis through an angle θ_x is described by (Eq. (1)):

$$\mathbf{p}_x = R(\theta_x) \cdot \mathbf{p} \quad (1)$$

$$\text{where } R(\theta_x) = \begin{bmatrix} 1 & 0 & 0 \\ 0 \cos(\theta_x) & -\sin(\theta_x) & \\ 0 \sin(\theta_x) & \cos(\theta_x) & \end{bmatrix}$$

Similarly, a rotation of a position vector \mathbf{p} about the y-axis through an angle θ_y is performed by the matrix operation (Eq. (2)):

$$\mathbf{p}_y = R(\theta_y) \cdot \mathbf{p} \quad (2)$$

$$\text{where } R(\theta_y) = \begin{bmatrix} \cos(\theta_y) & 0 & \sin(\theta_y) \\ 0 & 1 & 0 \\ -\sin(\theta_y) & 0 & \cos(\theta_y) \end{bmatrix}$$

Also, a rotation of a position vector \mathbf{p} about the z-axis through an angle θ_z is performed by the matrix operation (Eq. (3)):

$$\mathbf{p}_z = R(\theta_z) \cdot \mathbf{p} \quad (3)$$

$$\text{where } R(\theta_z) = \begin{bmatrix} \cos(\theta_z) & -\sin(\theta_z) & 0 \\ \sin(\theta_z) & \cos(\theta_z) & 0 \\ 0 & 0 & 1 \end{bmatrix}$$

Therefore, the rotation about the fixed axes x, y, and z in that order is described as (Eq. (4)):

$$\mathbf{p}_{xyz} = R(\theta_z) \cdot R(\theta_y) \cdot R(\theta_x) \mathbf{p} \quad (4)$$

However, if the rotations are defined about floating axes (ie the axes about which a vector rotates is rotated by the previous transformation) in the sequence x, y and then z, the rotation is described as (Eq. (5)):

$$\begin{aligned} \mathbf{p}_{xyz} &= R(\theta_x) \cdot R(\theta_y) \cdot R(\theta_z) \mathbf{p} \\ \mathbf{p}_{xyz} &= E_{xyz} \cdot \mathbf{p} \end{aligned} \quad (5)$$

where $E_{xyz} =$

$$\begin{bmatrix} \cos(\theta y) \cdot \cos(\theta z) & -\cos(\theta y) \cdot \sin(\theta z) & \sin(\theta y) \\ \cos(\theta x) \cdot \sin(\theta z) + \cos(\theta z) \cdot \sin(\theta x) \cdot \sin(\theta y) & \cos(\theta x) \cdot \cos(\theta z) - \sin(\theta x) \cdot \sin(\theta y) \cdot \sin(\theta z) & -\cos(\theta y) \cdot \sin(\theta x) \\ \sin(\theta x) \cdot \sin(\theta z) - \cos(\theta x) \cdot \cos(\theta z) \cdot \sin(\theta y) & \cos(\theta z) \cdot \sin(\theta x) + \cos(\theta x) \cdot \sin(\theta y) \cdot \sin(\theta z) & \cos(\theta x) \cdot \cos(\theta y) \end{bmatrix}$$

where E_{xyz} is the transformation matrix through the angles of θx , θy and θz about the floating x, y, z axes in that sequence. E_{xyz} also represents the projection of one co-ordinate system into another.

Therefore, if the transformation matrix from segmental reference frame to the orientation of a target reference frame is known it can be seen that (Eqs. (6-8)):

$$\theta y = \sin^{-1}(E_{xyz}(1,3)) \tag{6}$$

$$\theta x = \sin^{-1}\left(\frac{-E_{xyz}(2,3)}{\cos(\theta y)}\right) = \cos^{-1}\left(\frac{E_{xyz}(3,3)}{\cos(\theta y)}\right) \tag{7}$$

$$\theta z = \sin^{-1}\left(\frac{-E_{xyz}(1,2)}{\cos(\theta y)}\right) = \cos^{-1}\left(\frac{E_{xyz}(1,1)}{\cos(\theta y)}\right) \tag{8}$$

where θx , θy and θz are the Euler angles about the x , y , and z axes respectively.

References

- An, K.N.; Kwak, B.; Chao, E.; Morrey, B. 1984. Determination of muscle and joint forces: A new technique to solve the indeterminate problem, *Transactions of the American Society of Mechanical Engineering* 106: 364-367.
- Brand, R.; Crowninshield, R.; Wittstock, C. 1982. A Model of Lower Extremity Muscular Anatomy, *Journal of Biomechanical Engineering*, 104 (4): 304-310.
- Brand, R.; Pedersen, D.; Friederich, J. 1986. The Sensitivity of Muscle Force Predictions to Changes in Physiological Cross-Sectional Area, *Journal of Biomechanics*, 19 (8): 589-596.
- Breteler, K.; Spoor, C.; Van-Der-Helm F. 1999. Measuring Muscle and Joint Geometry Parameters of a Shoulder for Modeling Purposes, *Journal of Biomechanics*, 32 (11): 1191-1197.
- Chow, D.H.; Cheng, I.Y.; Holmes, A.D.; Evans, J.H. 2005. Muscular and centre of pressure response to sudden release of load in symmetric and asymmetric stoop lifting tasks, *Applied Ergonomics* 36(1): 13-24.
- Cooper, G.; Ghassemieh, E. 2007. Risk assessment of patient handling with ambulance stretcher systems (ramp/winch), easi-loader, tail-lift) using biomechanical failure criteria, *Medical Engineering and Physics*, 29(7): 775-787.
- Erdemir, A.; McLean, S.; Herzog, W.; Van den Bogert, A. 2007. Model based estimation of muscle forces exerted during movements, *Clinical Biomechanics* 22 (2): 131-154.
- Gracovetsky, S.; Farfan, H.; Lamy, C. 1977. A mathematical model of the lumbar spine using an optimization system to control muscles and ligaments, *Orthopaedic Clinics of North America*, 8 (1): 135-153.
- Grimshaw, P.N.; Marques-Bruna, P.; Salo, A.; Messenger, N. 1998. The 3-dimensional kinematics of the walking gait cycle of children aged between 10 and 24 months: cross sectional and repeated measures, *Gait Posture*, 7 (1): 7-15.

BIOMEHANIČKA ANALIZA ULASKA I IZLASKA IZ PUTNIČKOG VOZILA SA ZADNJIIM VRATIMA SA ZADNJIIM VEŠANJEM

James Shippen

Sažetak: U radu je sprovedena biomehantička analiza u cilju utvrđivanja artikulacije lumbalnog dela tela i opterećenja leđnih mišića prilikom ulaska i izlaska iz putničkog vozila sa vratima sa prednjim i zadnjim vešanjem. Takođe, istražena je mogućnost smeštanja i uzimanja predmeta sa zadnjeg sedišta putničkih automobila sa vratima sa prednjim vešanjem i vratima sa zadnjim vešanjem. Rezultati istraživanja su pokazali da su opterećenja leđnih mišića i uglovi artikulacije manji u slučaju vozila opremljenih sa vratima sa zadnjim vešanjem nego u slučaju istog modela vozila sa vratima sa prednjim vešanjem.

Ključne reči: biomehantička analiza, model celog tela, modeliranje mišića, vrata sa zadnjim vešanjem.